Discrete lattice solitons: properties and stability

1989 J. Phys. A: Math. Gen. 22 783

(http://iopscience.iop.org/0305-4470/22/7/011)

J. Phys. A: Math. Gen. 22 (1989) 783-801. Printed in the UK

Discrete lattice solitons: properties and stability

N Flytzanis†‡, St Pnevmatikos† and M Peyrard†§

† Research Center of Crete, PO Box 1527, 711 10 Heraklio, Crete, Greece
‡ Physics Department, University of Crete, 711 10 Heraklio, Crete, Greece
§ Laboratoire ORC, University of Bourgogne, 6 Bd Gabriel, 21100 Dijon, France

Received 2 August 1988

Abstract. We present a detailed numerical study of the dynamics of high-energy kink excitations in monatomic chains, with a simple description using a microscopic model of the narrow kink core. We present velocity-amplitude and energy-momentum curves for the kink which fit well the numerical results. Kink-kink collisions are slightly inelastic depending on the velocities and point of collision within a lattice spacing.

1. Introduction

Non-linear wave propagation in one-dimensional anharmonic lattices has been extensively studied for simple interatomic potentials of polynomial form (Fermi *et al* 1965, Zabusky 1973, Pnevmatikos 1983, 1985, Flytzanis *et al* 1985, 1987, Pnevmatikos *et al* 1986) which can approximate any realistic potential near the equilibrium separation distance of two atoms. This description, done usually in the continuum limit, is sufficient for small relative displacements from equilibrium. For non-linear waves with large relative displacements the interatomic potentials in real crystals can be better fitted by Morse, Lennard-Jones and other empirical potentials. The propagation of non-linear waves in more realistic potentials has mainly been studied numerically (Rolfe *et al* 1979, Ali and Somorjai 1979, Valkering and de Lange 1980). Some approximate analytic solutions have been obtained in the continuum approximation, valid for wide non-linear excitations for the cubic and quartic interaction potentials (Pnevmatikos 1985, Flytzanis *et al* 1985, 1987), for the (2, 1) Lennard-Jones potential (Yoshida and Sakuma 1979) or the more general $(2n, n)$ Lennard-Jones potential for $n = 2, 3, 4$ (Ishimori 1982). Significant improvement is obtained when using the quasicontinuum approximation (Collins 1981, Rosenau 1986). Exact analytic solutions, which are valid even for very narrow discrete excitations, can be obtained only for the Toda lattice, which is a discrete completely integrable system (Toda 1975).

In our previous studies (Peyrard *et al* 1986) we have shown that narrow soliton-like excitations can propagate in discrete monatomic chains without any energy loss due to discreteness effects. So, it is interesting to study highly discrete (i.e. very narrow) localised excitations in a lattice and investigate the possibility of soliton-like waves or even exact solitons in lattices with interaction potentials other than the Toda potential. At the same time we can check the limits for the validity of the existing continuum or quasicontinuum theories.

0305-4470/89/070783+19$02.50

In addition to the mathematical aspect of this problem, the study of narrow excitations is very important for specific physical applications such as, for instance, detonation waves in solids. A detonation wave is a highly supersonic wave sustained by the energy released in an exothermic chemical reaction, and the lattice compression can be as large as half the lattice spacing, while the detonation front can be extremely narrow. Recent studies have dealt both with the microscopic mechanism of the initiation of detonations and the propagation of the detonation in a molecular model using techniques from molecular dynamics (Hardy and Karo 1978, Peyrard *et al* 1985, Tsai and Trevino 1984). Several studies of shock waves in solids (Tasi 1980, MacDonald and Tsai 1978, Batteh and Powell 1978) under impact conditions have shown the importance of coherent non-linear excitations in the structure of the narrow shock front. These coherent excitations are the cause of the non-attainment of thermal equilibrium in a large domain behind the shock (MacDonald and Tsai 1978, Batteh and Powell 1978) which can persist even at non-zero lattice temperatures (Batteh and Powell 1978, Straub and Holian 1979). A detailed analysis of shock propagation in a one-dimensional Toda lattice has shown that the leading edge of the shock wave is well represented quantitatively by a single isolated soliton while following it is a slowly varying soliton wavetrain whose structure depends on the driving velocity of the piston causing the shock (Holian *et al* 1981).

The aim of this paper is to show that the narrow soliton-like excitations exhibited in our previous work (Peyrard *et al* 1986) exist in a large variety of non-linear lattices. We describe their dynamical behaviour and their characterisation via the appropriate amplitude–velocity relation and an investigation of the conserved quantities, such as energy, momentum, etc. In § 2 we present some analytical results valid mainly in the continuum approximation and describe briefly the effect of the lattice for discrete solitons. In § 3 we characterise the high-energy (narrow) excitations by introducing a simple model with a few particles near the soliton core and a fitting procedure using the analytical expressions for the Toda soliton with independent parameters for the amplitude, velocity and width. We also define the soliton momentum (distinguished from the chain momentum) as the congugated canonical variable to the soliton position and present its relation to the soliton energy. In § 4 we discuss the numerical results and in the final section we present a summary and our conclusions.

2. Continuum and lattice solitons

2.1. Interaction potentials

We consider a one-dimensional monatomic lattice with mass m, lattice spacing D and only nearest-neighbour interactions (NNI). The restriction to NNI is for simplicity and the results are easily extended to second and higher neighbours. The Hamiltonian of the system can be written in the general form

$$H = \sum_n [\tfrac{1}{2}m\dot{y}_n^2 + V(y_n - y_{n-1})] \tag{2.1}$$

where y_n is the atomic displacement from equilibrium, and the bond strain is

$$r_n = y_n - y_{n-1}. \tag{2.2}$$

The potential $V(r)$ can be quite general, but in this paper we limit ourselves to the following forms.

(i) Cubic-quartic:

$$V(r) = \tfrac{1}{2}Gr^2 + \tfrac{1}{3}Ar^3 + \tfrac{1}{4}Br^4 \tag{2.3}$$

with particular cases $B = 0$ or $A = 0$.

(ii) Morse:

$$V(r) = P(e^{-\alpha r} - 1)^2 \tag{2.4}$$

or a modification of it used by Collins (1981) with an extra parameter that changes qualitatively the attractive part of the interaction potential.

(iii) 12-6 Lennard-Jones:

$$V(r) = \varepsilon\left[\left(\frac{D}{D+r}\right)^{12} - 2\left(\frac{D}{D+r}\right)^{6} + 1\right]. \tag{2.5}$$

(iv) Toda potential:

$$V(r) = a\, e^{-br}/b + ar - a/b \tag{2.6}$$

which is used as a reference point for our results.

In all the above cases the parameters in the interaction potential can be determined by fitting to first principles calculations. In our case we examined a large range of numerical values for these parameters. The potentials are defined so that $V(0) = 0$.

The equation of motion for y_n can be written as

$$\frac{m\, d^2 y_n}{dt^2} = -V'(y_n - y_{n-1}) + V'(y_{n+1} - y_n) \tag{2.7}$$

or

$$\frac{m\, d^2 r_n}{dt^2} = V'(r_{n+1}) - 2V'(r_n) + V'(r_{n-1}) \tag{2.8}$$

for the strain r_n, where $V'(r) = dV/dr$. Except for the Toda lattice, which is exactly solvable, one must consider approximate solutions of (2.7) in the long-wavelength limit. These solutions can be used as initial conditions in numerical simulations for the study of narrow kinks.

2.2. Approximate continuum solutions for the lattice solitons

In the usual continuum approximation, with $x = nD$ a continuum variable, we expand the finite-difference operator in the RHS of (2.7) or (2.8) as

$$V'(r_{n+1}) - 2V'(r_n) + V'(r_{n-1}) \simeq D^2 \frac{\partial^2 V}{\partial x^2} + \tfrac{1}{12}D^4 \frac{\partial^4 V}{\partial x^4} \tag{2.9}$$

where $V' = V'(r(x))$ and we neglect higher derivatives. If one keeps only the linear term for r in the second term of the RHS of (2.9), then for the potential (2.3) one obtains the generalised Boussinesq (GBq) equation from (2.7) for $u = y_x$:

$$u_{tt} - c_0^2 u_{xx} - p(u^2)_{xx} - q(u^3)xx - hu_{xxxx} = 0 \tag{2.10}$$

with

$$\begin{aligned} c_0^2 &= GD^2/m & p &= AD^3/m \\ h &= GD^4/(12m) & q &= BD^4/m. \end{aligned} \tag{2.11}$$

The analytical solutions for (2.10) are given in the appendix, and here we summarise the results. For NNI only, $h>0$ so that we always have supersonic excitations with velocity $v>c_0$. For B (or q) <0 there are no excitations, except when with second-neighbour interactions we have $h<0$ and then there are no kink excitations for $B>0$. For $B>0$ with $A\neq 0$ there are both compressive and rarefactive kinks, but in the continuum approximation only the kink that has the same sign as A (or p) is stable. This point will be examined later for more general potentials. For $B>0$ and $A=0$ both compressive and rarefactive kinks are stable. Since the empirical pair potentials have $A<0$ when expanded near the equilibrium position the kinks are compressive and feel the repulsive part of the potential.

Even in the continuum approximation no analytic solution exists for the Morse potential. For the (2-1) Lennard-Jones lattice with NNI an analytic expression has been obtained (Yoshida and Sakuma 1979) without expanding the non-linear potential in powers of r, except that in the dispersive term only the linear part of the potential is considered.

In the quasicontinuum approximation (Collins 1981, Rosenau 1986) one inverts the finite-difference operator instead of expanding it and obtains an integro-differential equation. If one looks for a solution of the form $y(x-vt)$ the same result as the GBq equation in (2.10) is obtained, but with a different dispersion parameter $h_1=hv^2/c_0^2$ which depends now on the velocity. If v is near c_0, of course, then h reduces consistently to the continuum approximation value where the width also goes to infinity. Again, no analytic solutions exist for the Morse or Lennard-Jones potentials. Even in this improved approximation of the quasicontinuum the known analytic solutions break down when the width of the excitations is comparable to the lattice spacing.

2.3. Effect of discreteness

The dynamical effects of the discrete lattice for narrow excitations has been studied for dislocations (Flytzanis *et al* 1977, Flytzanis 1978, Earne and Weiner 1974) and topological solitons of the sine-Gordon type (Peyrard and Kruskal 1984). In this case the excitation will 'feel' the lattice and lose energy by radiation of small amplitude waves.

In the case of non-topological solitons we have shown (Peyrard *et al* 1986) that for a monatomic chain there is energy loss for subsonic excitation but not for supersonic excitation. Due to coherence of the motion the emission occurs at specific frequencies, such that the phase velocity of the emitted radiation is equal to the soliton velocity and we have constructive interference, i.e.

$$\omega(k)/k=v \tag{2.12}$$

where $\omega(k)$ is the linear dispersion relation. Condition (2.12) is never satisfied for supersonic solitons at finite k. From this we expect that narrow soliton-like excitations will propagate undamped as was already checked for simple cases. Here we generalise these results for general interaction potentials and determine the properties of these excitations. The above condition for emission has been verified for subsonic solitons or for solitons in diatomic chains (Peyrard *et al* 1986). The emission arguments break down for wide solitons since the amplitude of the emitted waves is modulated by a function that drops exponentially with large widths, so that the continuum approximation results are valid.

3. Properties of highly discrete lattice solitons: numerical results

3.1. The numerical method

Since no exact analytic solutions exist we have developed a procedure to obtain them numerically using the non-linear chain as a 'soliton generator' with some appropriate initial conditions. The starting excitation is obtained from the continuum approximation (see appendix) extending the parameter for the width to values of the order of the lattice spacing. Some improvement is obtained by using the result of the quasi-continuum approximation, but in both cases the velocity of the emerging excitation for a given amplitude is very different after propagation.

The coherent excitation separates from the transient after propagation on the chain, since the kink is supersonic while the oscillations move at the speed of sound. The separated kink emits no radiation in agreement with our prediction. When the kink is clearly separated from the transient, the part of the chain containing the transient is removed and we study the properties of the 'pure' kink. The emerging excitation is called a 'lattice soliton' to distinguish it from solitons derived from the continuum or quasicontinuum approximations. The fact that the chain is able to create such a solitary excitation from rather different initial conditions is an indication of the stability of these excitations, and therefore they should play a role in physical situations where shocks are involved.

The numerical scheme for solving the non-linear differential-difference equations of motion is a fourth-order Runge–Kutta method on a lattice with 500 atoms and fixed boundary conditions as described earlier (Pnevmatikos 1985, Peyrard *et al* 1986).

3.2. Analysis of the soliton profile

A detailed numerical study of the 'lattice soliton' propagation shows oscillations in kinetic and potential energy with a period of one lattice spacing, while the total energy, of course, is constant. These oscillations are large and exist also in the Toda lattice due to the finite number of particles (in some cases two or three) in the soliton core. The question arises whether part of these oscillations can be due to shape fluctuations or velocity oscillations. This is the case with topological solitons (Ishimori and Munakata 1982) that feel the Peierls barrier of the static substrate which is absent in our model.

The study of the motion within a lattice spacing requires a careful determination of the soliton position. A simple linear interpolation between core atoms is not sufficient, and velocity fluctuations caused by the roughness of the position determination are observed. Other polynomial fittings do even worse. The method we have chosen is to fit the numerical values for $y_n(t)$ by a modified function of a Toda soliton in which the amplitude A_m and width w can vary independently:

$$y_F(x) = \tfrac{1}{2}A_m^w \ln\left(\frac{1+\exp[\pm 2(x-x_0-\frac{1}{2})/w]}{1+\exp[\pm 2(x-x_0+\frac{1}{2})/w]}\right) + \text{constant} \tag{3.1}$$

where x_0 is the soliton position. The $\pm$ sign is introduced to also allow for the fitting of rarefactive solitons that do not exist for the Toda lattice. The parameter A_m can be considered to be known, since $A_m = y(\infty) - y(-\infty)$. The fitting with (3.1) is very good, as can be seen in figure 1 and the parameters x_0 and w are evaluated. During propagation within a unit cell the width and velocity of the excitation remain constant

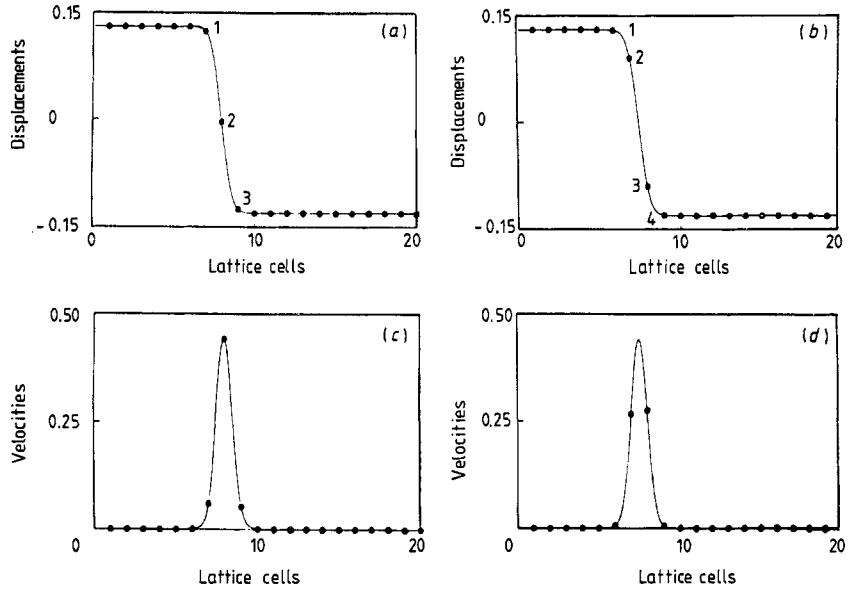

Figure 1. Fitting with a Toda type function from (3.1) for the atomic displacement for two configurations A and B, shown in (a) and (b), where the kink is centred on a particle or between two particles respectively. The corresponding velocities are fitted in (c) and (d).

to within a relative error of 10^{-2} (10^{-4} for the Toda lattice). Thus, it is meaningful to write $y_n(t) = f(n - vt)$ where $f(x)$ is a well defined smooth function and v the soliton velocity. For narrow excitations it is difficult to define the width, but the choice of (3.1) makes $2w$ a natural candidate for the full width.

3.3. Amplitude-velocity relation

Numerical simulations have shown that the amplitude of the lattice soliton which emerges from a continuum (or quasicontinuum) initial condition is very different from the initial amplitude for very narrow solitons. We have undertaken a study of the soliton amplitude-velocity relation in two cases: (i) power law interatomic potentials for which there are analytic expressions in the continuum approximation to compare with, and (ii) more physical potentials (Morse, Lennard-Jones etc) to investigate the effect of the potential shape.

In figure 2 we plot the kink amplitude ($A_m < 0$) as a function of velocity for a cubic potential with $G = 1$, $A = -10.5$, and $B = 0$ in (2.3). The points are the experimental results fitted by a discrete method (DM) valid at large amplitudes (the continuous curve) to be described in § 4. The kinks are compressive in the whole range of velocities, in full agreement with previous results (Pnevmatikos 1983, Flytzanis *et al* 1985). The continuum approximation (CA) result is given by

$$A_m = 6[h(v^2 - c_0^2)]^{1/2}/A \qquad \text{CA} \tag{3.2a}$$

with h and c_0 given by (2.11), and is qualitatively different from our results. The quasicontinuum approximation (QCA) for which

$$A_m = 6v[h(v^2 - c_0^2)]^{1/2}/(c_0 A) \qquad \text{QCA} \tag{3.2b}$$

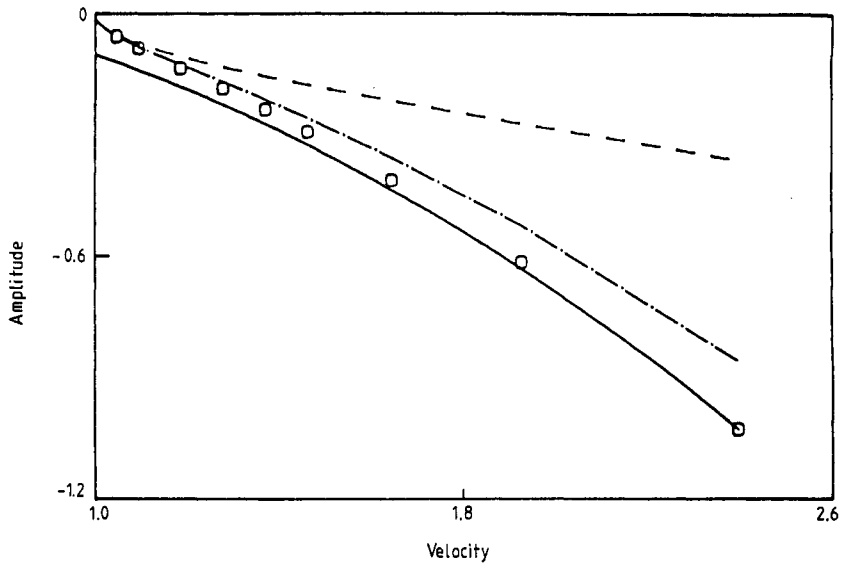

Figure 2. Amplitude-velocity plot for a cubic potential ($G = 1$, $A = -10.5$, $B = 0$). Numerical points (circles); continuum approximation (broken curve); quasicontinuum approximation (chain curve); discrete description (full curve).

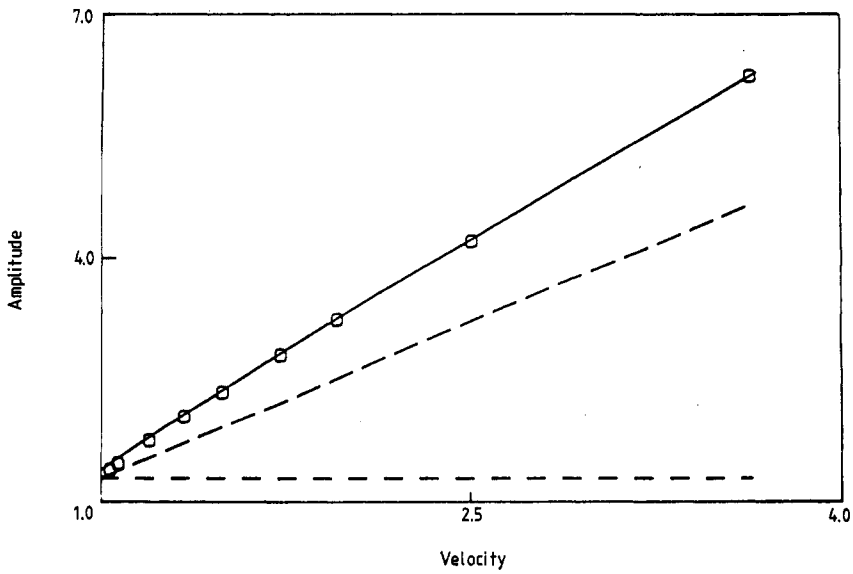

Figure 3. Amplitude-velocity plots for a quartic potential ($G = 1$, $A = 0$, $B = 1$). See caption in figure 2.

is better, but does not fit correctly the experimental points at large amplitudes. In figure 3 the amplitude-velocity relation is presented for a quartic potential with $G=1$, $B=1$ and $A=0$. The CA and QCA results are respectively

$$A_m = 4(2h/B)^{1/2} \qquad \text{CA} \tag{3.3a}$$

and

$$A_m = 4v(2h/B)^{1/2}c_0 \qquad \text{QCA} \tag{3.3b}$$

so that in (3.3*a*) A_m is independent of v while in (3.3*b*) we have the wrong slope. On the contrary, the discrete method gives a perfect fit. Due to the symmetric potential we have both compressive and rarefactive solitons. The compressive excitations have a meaning when A_m is less than a lattice spacing. For realistic values of B it is generally possible, since the amplitude at $v \simeq c_0$ is inversely proportional to the square root of B (see appendix).

In figure 4 we present the amplitude-velocity relation for a cubic-quartic potential with $G=1$, $A=-10.5$ and $B=62$ chosen so that the potential is a good fit to a Morse potential near equilibrium for a particular material (Ag). In figure 4(*a*) for compressive kinks, the CA result is not good, while the QCA and DM fit respectively the small and high amplitude regions. At small amplitudes the behaviour corresponds to a cubic potential while at high amplitudes to a quartic. In figure 4(*b*) we present the rarefactive kink results which are perfectly fitted by the DM description. Both the CA and QCA are bad fits in this case. For v near c_0 the continuum solution is unstable since the width is of the order of the lattice spacing, which is inconsistent with the CA. The continuum solution is not a good starting point for the simulations and near $v \simeq c_0$ the CA amplitude is multiplied by a factor so that the elastic energy is considerably increased. The CA result for A_m is

$$A_m = 4(2h/g)^{1/2}\tan^{-1}(1/w) \qquad \text{CA} \tag{3.4}$$

with w given in (A2), which at $v=c_0$ reduces to $2\pi(2h/q)^{1/2}$ and is independent of A. The limit $A \to 0$ does not reproduce the quartic potential result (3.3) for which we must take the limits $A \to 0$ and $v \to c_0$ in the correct order. In either case the numerical results are different. For higher velocities the rarefactive excitations are easily attainable numerically.

In order to investigate the effect of the form of the potential we started with the Morse potential for Ag, which has a mass $m = 107.87m_0$ where m_0 is taken as the mass unit, and lattice spacing $D = 3.225$ Å taken to be the unit of length. The parameters in the Morse potential are $\alpha = 1.369$ Å^{-1} and $p = 0.3323$ eV. If we use as the energy unit $E_0 = 1$ eV, the time unit is defined as $t_0 = (m_0D^2/E_0)$ while the speed of sound $c_0 = 3276$ ms^{-1} is very reasonable. In table 1 we give the parameters chosen for the other potentials as well as their force constants when expanded in a Taylor series such that the expansion coefficients G, A and B are approximately equal (see figure 5).

In figure 6 we plot the kink amplitude versus velocity for all four potentials. The curves match for velocities near the speed of sound, as expected, due to the choice of matching of the bottom of the potential wells. For higher velocities the curves diverge from each other and follow in order of increasing steepness of the potentials for the range of amplitudes studied.

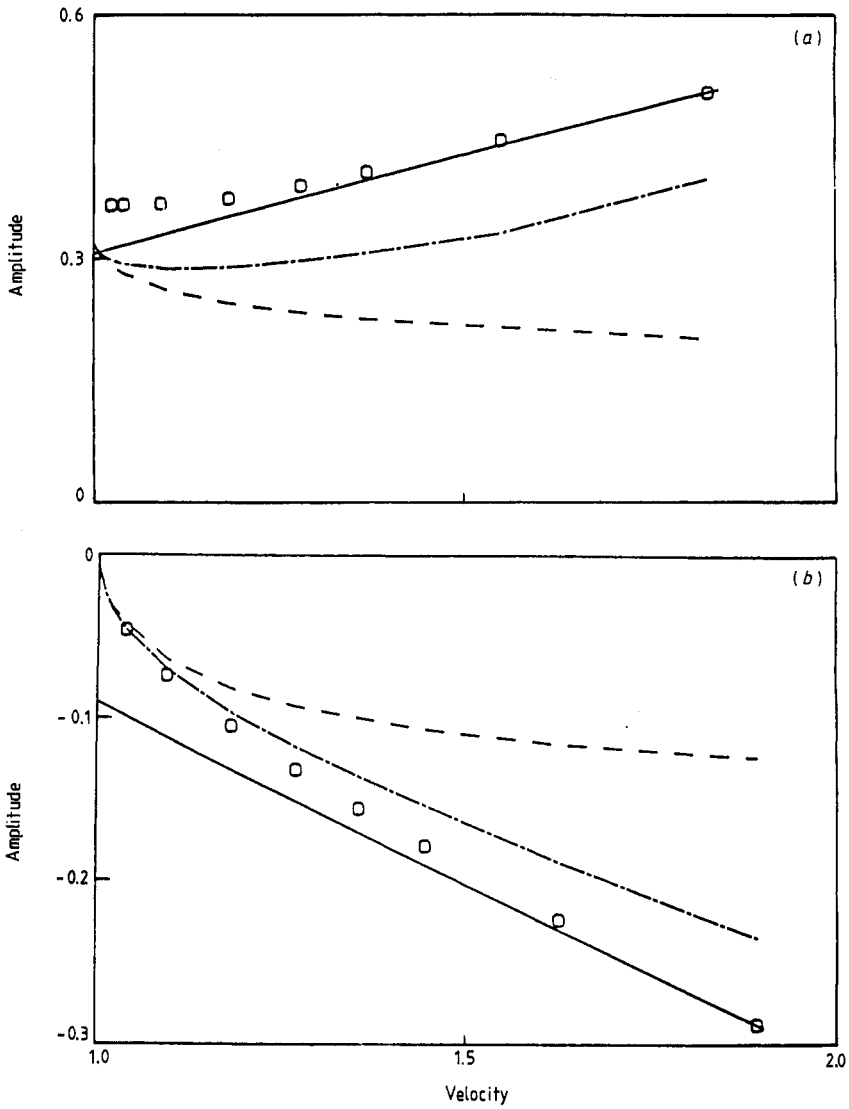

Figure 4. Amplitude-velocity plots of (*a*) rarefactive and (*b*) compressive solitons for a cubic-quartic potential ($G=1$, $A=-10.5$, $B=62$). See caption in figure 2.

Table 1.

Potential parameters		Power law expansion		
Cubic-quartic		$G_1=1$	$A_1=-10.5$	$B_1=62$
Morse	($a=7$, $P=0.01$)	$G_1=1$	$A_1=-10.5$	$B_1=57$
L-J	($\varepsilon=0.013\,89$)	$G_1=1$	$A_1=-10.5$	$B_1=62$
Toda	($ab=1$, $b=21$)	$G_1=1$	$A_1=-10.5$	$B_1=73.5$

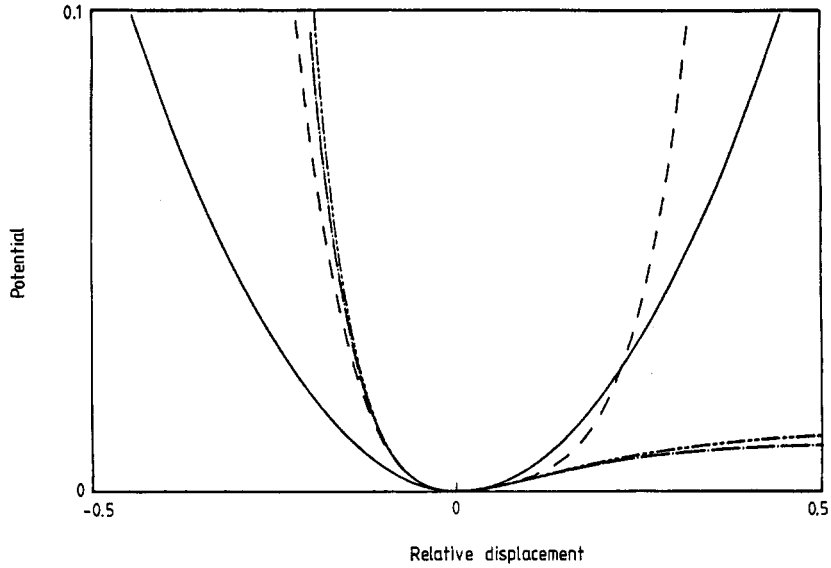

Figure 5. Interatomic potentials for the parameters given in table 1: harmonic (full curve); cubic-quartic (broken curve); Morse (chain curve); Lennard-Jones (double-dot chain curve).

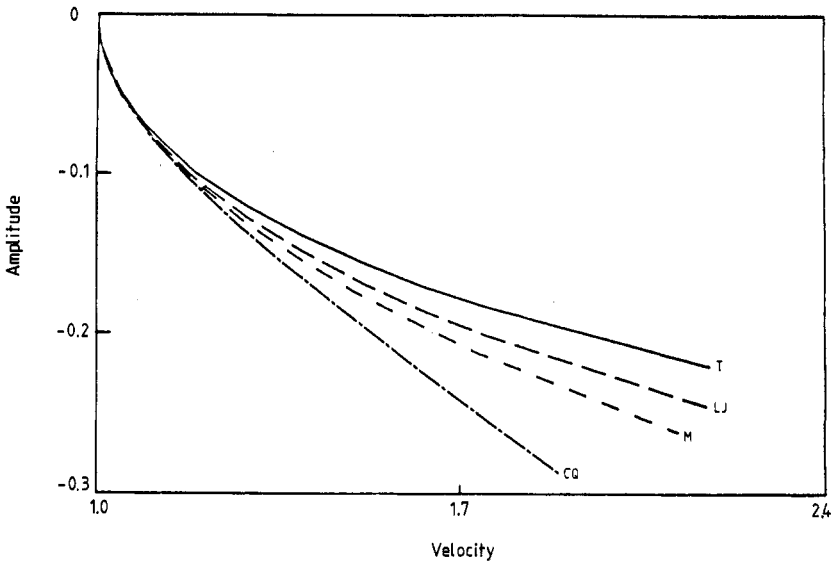

Figure 6. Comparison of amplitude-velocity numerical curves for the cubic-quartic (CQ), Morse (M), Lennard-Jones (LJ) and Toda (T) potentials with parameters given in table 1.

3.4. Energy-momentum relation

The total energy and momentum of the atomic chain are conserved and given by

$$E_{\text{tot}} = \sum_{n=1}^{N} \left(\frac{p_n^2}{2m} + V(y_{n+1} - y_n) \right) \tag{3.5}$$

$$P_c = \sum_{n=1}^{N} p_n \tag{3.6}$$

where p_n is the momentum of the nth particle and N is the number of particles. The chain momentum P_c is the momentum canonical to the centre of mass of the chain coordinate which is at rest for an infinite chain. Since we consider excitations travelling at a constant velocity v we can define the soliton position coordinate $x_0(t)$, and its corresponding conjugate momentum P_s given by (Mertens and Büttner 1982)

$$dP_s(E)/dE = \pm 1/v(E) \tag{3.7}$$

where E is the total energy of the soliton. Equivalently, for a single soliton, P_s can be defined as the action variable

$$P_s = \sum_{n=1}^{N} \oint m\dot{y}_n \, dy_n = \sum_{i=1}^{N} \int_0^T m\dot{y}_n^2(t) \, dt \tag{3.8}$$

where the integral should be taken over the phase space trajectory of the nth particle, when the soliton moves one lattice spacing, i.e. $T = D/v$. Explicit calculation for the Toda lattice has verified the consistency of (3.7) and (3.8) and it is P_s, not P_c, which gives the correct description for the statistical mechanics of the system (Mertens and Büttner 1982) in the picture of an ideal gas of solitons. Expression (3.8) is essentially the average of the total kinetic energy over the period $T = D/v$. For a single soliton this should be equivalent to the kinetic energy of a single atom integrated over all times:

$$P_s = m \int_0^{\infty} \dot{y}_n^2(t) \, dt. \tag{3.9}$$

In the continuum limit the corresponding quantities can be easily calculated since analytic expressions are known (cubic, quartic potential etc) for the soliton form. If we define the basic units of length λ_x, time λ_t and energy λ_e as

$$\lambda_x = (h/c_0^2)^{1/2} \qquad \lambda_t = (h/c_0^4)^{1/2} \qquad \lambda_e = 6^2 m \lambda_x c_0^6/(pD) \tag{3.10}$$

for the cubic potential, we have for a single soliton (Flytzanis *et al* 1987)

$$E_{tot} = \lambda_e(\tfrac{2}{3}k^3 + \tfrac{2}{3}k\Omega^2 + \tfrac{24}{15}k^5) \tag{3.11}$$

$$P_c = M_s v = M_s c_0 \Omega/k \tag{3.12}$$

$$P_s = \lambda_e(\tfrac{4}{3}\Omega k^2)/c_0 \tag{3.13}$$

where M_s is the soliton mass

$$M_s = -12kM_0 = -12kmc_0\sqrt{h}/Dp \tag{3.14}$$

and

$$\Omega^2 = k^2 - 4k^4 \tag{3.15}$$

where k and Ω/k are the dimensionless inverse width and velocity, respectively, of the soliton (Flytzanis *et al* 1987). Using (3.11) and (3.12) for E_{tot} and P_s respectively, relation (3.7) is easily verified, as is also the case for the quartic and the discrete Toda lattice (Mertens and Büttner 1982).

It is very important in the energy in (3.11) to include all the terms up to some order in k (i.e. k^5) and not just take one of the conserved quantities for the Boussinesq equation (Flytzanis *et al* 1987) which includes the main part of the energy.

In figure 7 we plot the energy E_{tot} against the soliton momentum P_s for a cubic potential ($G=1$, $A=-10.5$, $B=0$). E_{tot} and P_s are measured numerically. At low energies (or velocities) the points are well fitted by the continuum approximation result from (3.11) and (3.13), where E_{tot} and P_s are given parametrically. At higher energies, as expected, the deviation is quite large and the quasicontinuum approximation does not change the curve since both E_{sol} and P_s are multiplied by the same factor v/c_0.

In figure 8 we plot E_{tot} against P_s for the Morse potential given in table 1 and the points are fitted by two curves to be discussed in § 4.

3.5. Lattice soliton collisions

In the previous sections we demonstrated that stable narrow lattice solitons exist for most interatomic potentials. Here we will investigate in more detail their soliton behaviour by studying numerically their collision properties. In general the collision is inelastic, as shown in figure 9 for a kink-kink collision, but the degree of inelasticity varies strongly and can even be zero as will be discussed below.

In figure 10 for a quartic potential ($G=1$, $A=0$, $B=62$) we plot the percentage of energy loss after a soliton scattering between a rarefactive and compressive excitation of opposite velocities ($v=2.8c_0$) as a function of the position of collision inside a lattice spacing. We see that for the extremely narrow kinks the collision is almost elastic if it happens between two particles, while the inelasticity takes its maximum when the collision happens on a particle. In the limit of very narrow excitations the elastic kink collisions correspond to two-particle collisions and the inelastic ones to three-particle collisions (Valkering and de Lange 1980). The form of the plot changes for different velocities.

The maximum percentage of energy loss in a kink-antikink collision (collision on a particle) is shown in figure 11 against the kink velocity. As v is near c_0 the collision

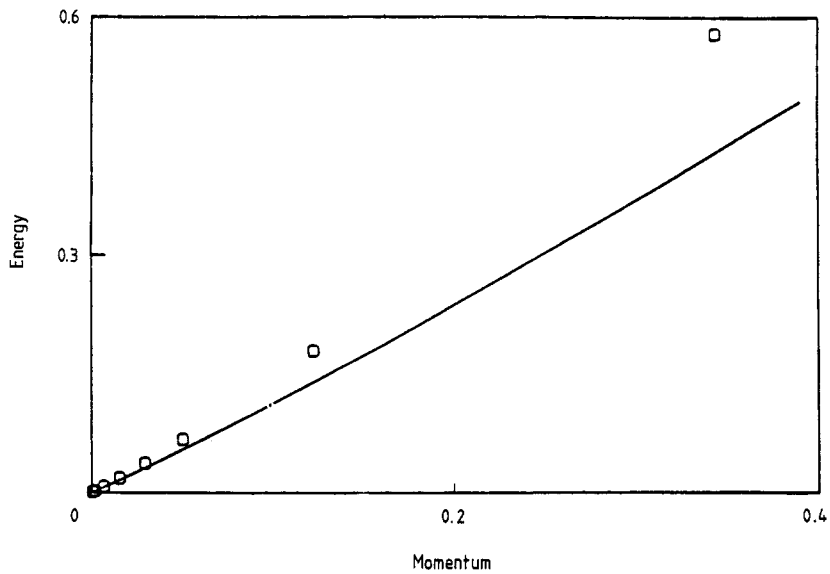

Figure 7. Total energy-momentum relation for a cubic potential ($G=1$, $A=-10.5$, $B=0$): numerical points (circles); continuum approximation (full curve).

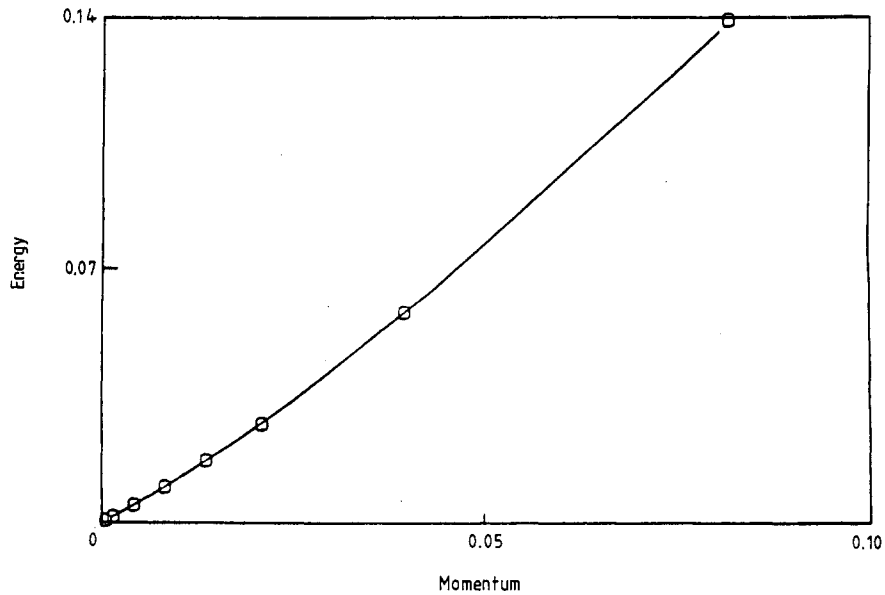

Figure 8. Total energy-momentum plot for the Morse potential of table I. Numerical points are compared with the result of (4.5) for E_{tot} and (4.8) for p_s using the fitting procedure in § 4.2 for $w = 0.456\,31$.

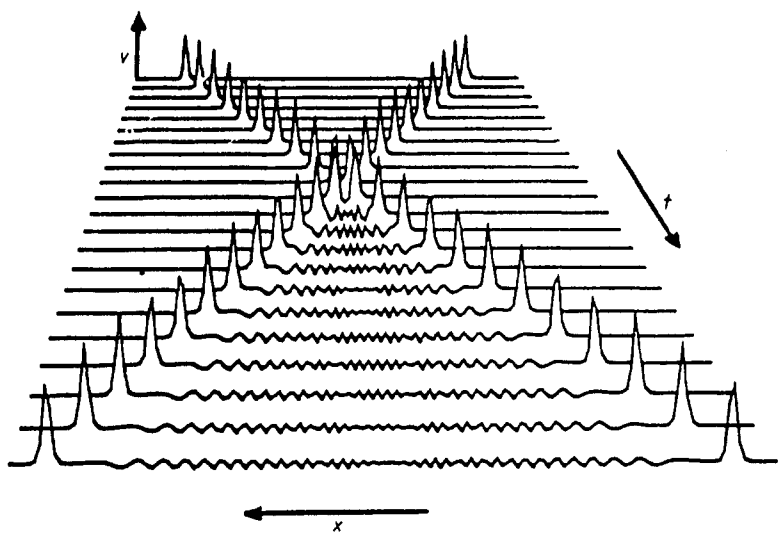

Figure 9. Particle velocities in a soliton-antisoliton collision ($v_1 = -v_2 = 1.855$) in a chain with quartic interactions ($B = 62$) for the maximum inelasticity case.

is elastic. As v increases the energy loss rises rapidly reaching a maximum of 7.8% at about $v = 1.4c_0$, after which it levels off at about 6.5%. The curve seems to be rather independent of the value of B in the quartic potential since in figure 11 the points obtained for $B = 1$ or $B = 62$ sit on the same curve. The results of kink collisions are in agreement and complement the conclusions of Valkering and de Lange (1980) where a hard-sphere description was used.

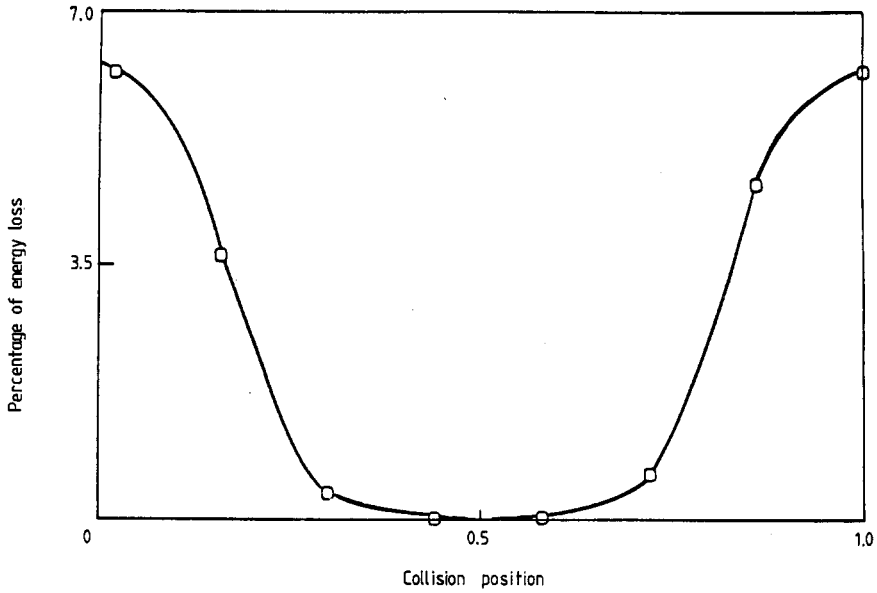

Figure 10. Percentage of energy loss for a kink-antikink collision against the position within a lattice spacing where the collision occurs.

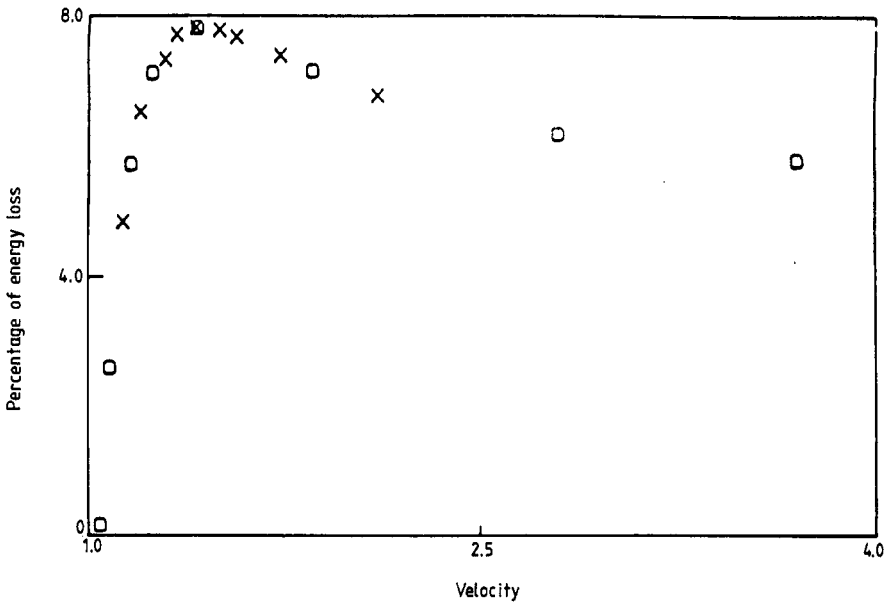

Figure 11. Percentage of energy loss after a kink-antikink collision for the maximum loss position (of the previous plot) versus the soliton velocity. The interaction potential is quartic $G=1$, $B=62$ (circles) and $B=1$ (crosses).

4. Discussion and analysis

4.1. Phenomenological description of the amplitude-velocity curve

In the absence of an analytic solution for the high-energy kinks we present a microscopic picture of the soliton dynamics by studying the motion of a few atoms near the core. During the uniform motion the displacement pattern changes periodically with a period equal to $\tau = D/v$. The motion interchanges between the configuration in figure 1(a) where one atom is at the centre and figure 1(b) where two atoms are involved. Applying energy conservation for the two configurations we can obtain an amplitude-velocity relation for the kink. We have

$$E_a = m\dot{y}_2^2/2 + 2V(A_m/2) \tag{4.1a}$$

$$E_b = 2(m\dot{y}_{2,3}^2/2) + V(A_m) + \Delta V \tag{4.1b}$$

where $\dot{y}_2$ is the velocity of the central atom in figure 1(a) and $\dot{y}_{2,3}$ is the velocity of atoms 2 or 3 in figure 1(b). In ΔV we can include the elastic energy for bonds (1-2) and (3-4), but for simplicity we consider the case where this is small, and we approximate the stretching of bonds (1-2) and (2-3) in figure 1(a) by $A_m/2$ and (2-3) in figure 1(b) by A_m. For a particular choice of potential this is possible approximately. Since we found in § 2 that the excitation can be described by a uniform function $f(n - vt)$ we can determine $\dot{y}_2$ if we know the slope of the continuum function written as A_m/L, i.e.

$$\dot{y}_2 = -vA_m/L \tag{4.2}$$

where L is a constant and is of the order of the soliton width. From momentum conservation we have

$$\dot{y}_{2,3} = \dot{y}_2/2. \tag{4.3}$$

Using (4.2) and (4.3) in (4.1) since $E_a = E_b$ we obtain

$$v^2 = (4L^2/A_m^2)[V(A_m) - 2V(A_m/2) + \Delta V] \tag{4.4}$$

for the amplitude-velocity relation, valid at high amplitude. In general, L is a function of velocity but varies very little, so that it is taken as constant. Equation (4.4) is fitted to the numerical results in figures 2-4. The parameter L is chosen by fixing the curve (4.4) on the highest velocity point. The value of L can also be checked by determining the function in (3.1) that fits the displacement $y_n(t)$ and obtain A_m/L from the slope at the centre. In all cases the value of L is very close to that obtained from fitting of (4.4) for the high-velocity region where ΔV is negligible. The fitting is quite reasonable and even excellent for the quartic potential where the soliton amplitudes are large even at velocities near c_0. At small amplitudes ($v \approx c_0$) the continuum approximation is more appropriate. If ΔV is not negligible then we can use the more accurate procedure presented in the next section. The drawback of this simple method is that we cannot obtain a fitting for the soliton energy-momentum relation since the evaluation of P_s involves a time integration from $\dot{y}_n$ over the period T.

4.2. Improved description of the energy-momentum curve

Since we need $\dot{y}_n(t)$ in (3.8) at all times, we perform a fitting for $y_n(t)$ with (3.1) and determine the parameters w and v, while the amplitude A_m is obtained directly. For

the energy in (4.1) we can include as many terms as necessary since there exists an analytic expression.

For the configurations in figures 1(a) and (b) we have

$$E_a = m\dot{y}_2^2/2 + 2(m\dot{y}_{1,3}^2/2) + 2V(r_{1,2}) \tag{4.5a}$$

$$E_b = (m\dot{y}_{2,3}/2) + V(R_{2,3}) + 2V(R_{1,2}) \tag{4.5b}$$

where $r_{i,j}$ and $R_{i,j}$ are the strains between the ith and jth atoms in the two configurations. In (4.5) for E_a we added the kinetic energy of the atoms 1 and 3, while in E_b we added the potential due to the strain $R_{1,2}$ which corresponds to ΔV in (4.1). If the kink is not very narrow these extra terms could be important. Using (4.1) we can evaluate the particle velocities and strains in (4.5) at times $t = 0$ and T. Equating E_a to E_b we obtain a relation between A_m and v, i.e.

$$v^2 = 4[V(R_{2,3}) + 2V(R_{1,2}) - 2V(r_{1,2})]/(Q^2 M A_m^2) \tag{4.6}$$

with

$$Q^2(w) = \left(\frac{2\sinh z}{1+\cosh z}\right)^2 + 4\left(\frac{e^z}{1+e^z} - \frac{e^{3z}}{1+e^{3z}}\right)^2 - \left(\frac{\sinh z}{\cosh z}\right)^2 \tag{4.7}$$

where for simplicity we defined $z = 1/w$. In (4.6) there is no adjustable parameter since everything is determined from (3.1) once w is evaluated. Equation (4.7) is a slight improvement over (4.4), but the price we pay is the fitting procedure necessary to evaluate w.

Using (3.1) for $y_n(t)$ and (3.8) we can evaluate the soliton momentum P_s as

$$P_s = \frac{A_m^2 v w}{\sinh(1/w)}\left(\frac{\cosh(1/w)}{w} - \sinh(1/w)\right) \tag{4.8}$$

where the dependence of P_s on the parameters A_m and v is very simple. This means that we can also determine w by evaluation of P_s from numerical integration of the equations of motion, and use (4.8) since A_m and v are easily determined from the simulation. Equation (4.8) reduces to the Toda expression if for A_m and v we use the relation for the Toda soliton. Using (4.5) and (4.8) we can fit the kink energy–momentum curves and the agreement is very reasonable by comparing the solid line with the numerical points in figure 8 for the Morse potential with parameters given in table 1. It should be remarked that the curve is not very sensitive to w. If, however, one chooses a slightly different w then the points still fall on the experimental curve but are displaced from the corresponding numerical points. The w obtained from the fitting also gives a point-by-point agreement.

5. Conclusions

In this paper we studied the properties of non-linear excitations in lattice dynamics whose width is comparable to the lattice spacing. As shown earlier, their propagation is possible in monatomic one-dimensional chains (Peyrard *et al* 1986) with no emission of lattice waves. We have shown here that these excitations are not perfect solitons since their collisions are quasi-elastic and the degree of inelasticity can vary considerably and can even be negligible. Their analytical description is much beyond the limits of validity of the continuum approximation or even the improved quasicontinuum

approximation. For this reason we used numerical methods to study the dynamics of these excitations for various interatomic potentials including Morse and Lennard-Jones as well as polynomial type potentials. We discussed their important characteristics with a simple microscopic model which involved only a few atoms in the highly-strained region of the kink. The numerical results obtained for the amplitude-velocity and energy-momentum relations are well described by the simple discrete approach, at high velocities when the kinks are very narrow. On the other hand, the continuum approximation seems to be valid only for $v = c_0$ and even in that case one must be careful for consistency of the solution (see § 3.3).

In agreement with earlier work (Rolfe *et al* 1979, Ali and Somorjai 1979) there are soliton-like excitations in monatomic chains with nearest-neighbour interactions for any interatomic potential as long as its repulsive part is more anharmonic than quadratic. We also add that there are large amplitude rarefactive solitons if the attractive part of the potential grows faster than quadratic in the vicinity of the equilibrium point (see figure 4*b*). This occurs for the exothermic type potentials used to model crystals for the propagation of detonations (Hardy and Karo 1978, Peyrard *et al* 1985). In fact, this is the case in Ali and Somorjai (1979) for a modified Morse potential where rarefactive solitons were observed numerically while they are unstable in the standard Morse potential (Rolfe *et al* 1979) as verified also in our simulations. So there is a simple explanation for the earlier disagreement. The range of velocities for which rarefactive solitons exist depends on the particular potential and of course could be zero.

In a chain with second-neighbour interactions which are additive to the nearest-neighbour interactions the conclusions are still valid. For strongly competitive interactions the solitons are subsonic and rarefactive for a simple Morse type potential (Pnevmatikos 1983, Flytzanis *et al* 1987). For velocities far from the speed of sound, however, there are discretisation effects due to the emission of lattice waves and only wide excitations are stable (Peyrard *et al* 1986). The effect of longer range forces has been studied analytically in the continuum approximation (Ishimori 1982, Remoissenet and Flytzanis 1985). In both cases the range of the interaction distance influences drastically the dispersive part of the equation of motion corresponding to (2.10).

Collisions between the narrow solitary excitations have small inelasticity and therefore the non-linear excitations have a long lifetime. This should be reflected in thermal conductivity numerical experiments. An extreme case is that of the discrete Toda lattice, which is a completely integrable system and shows infinite conductivity. The lack of thermalisation of energy is not seen in diatomic chains (Mokross and Büttner 1983) in accordance with our results where only the low-energy solitons are stable (Peyrard *et al* 1986) and high-energy solitons slow down by emitting lattice waves of optical frequencies (Peyrard *et al* 1986). This mechanism could contribute in part to the stochastic behaviour of the system, since there are other parameters that are important as the energy per particle of the chain, which in turn depends on the boundary conditions due to the constant temperature reservoirs at the chain ends. Also, collisions between kinks in a diatomic chain could be much more inelastic than that shown for a monatomic chain in figure 11, depending on their velocities.

The investigation of solitary wave excitation, propagation and decay is very important in understanding energy transfer and vibrational relaxation in coupled oscillator systems, both in one-dimensional chains and finite molecules. In this case, of course, one should also consider the high-energy periodic non-linear waves, which turn out to become unstable due to the onset of a chaotic behaviour when the oscillating solutions have energy densities which exceed a critical value, when the bond stretch

reaches the inflection point of the long-range part of the past interatomic potential (Collins and Rice 1982). The same can happen for the large amplitude oscillations during the collision of kinks.

Finally, the high-energy solitons are especially relevant for physical cases where large displacements are involved, such as shock waves and detonation waves. Even at non-zero temperatures computer simulations show the lack of thermalisation in the wake of the shock, while in the case of two or three dimensions a damping mechanism for the non-linear coherent excitations is provided, due to the coupling of transverse and longitudinal motions (Powell and Batteh 1980). The extent, however, of the thermalisation depends on the geometry of the two-dimensional lattice.

Acknowledgment

Part of this work has been supported by the Franco-Hellenic cooperation agreement and the CEE stimulation programme (no ST 2J-0032-1-GR). The authors acknowledge a useful contribution to § 3.5 by G Kastrinakis (University of Crete).

Appendix

From (2.10) the solution for the atomic displacement $y(x, t)$ is:

$$y(x, t) = \pm 2 \operatorname{sgn}(h)(2h/q)^{1/2} \tan^{-1}\{(1/w) \tanh[(x - vt)/L]\} \tag{A1}$$

with

$$w = \left(\frac{[4p^2 + 18(v^2 - c_0^2)q]^{1/2} \pm 2p}{[4p^2 + 18(v^2 - c_0^2)q]^{1/2} \mp 2p}\right)^{1/2} \tag{A2}$$

and

$$L = 2[h/(v^2 - c_0^2)]^{1/2}. \tag{A3}$$

For $q = 0$ (A1) becomes

$$y(x, t) = \operatorname{sgn}(h)\{2[h(v^2 - c_0^2)]^{1/2}/p\} \tanh[(x - vt)/L] \tag{A4}$$

and for $p = 0$ we have

$$y(x, t) = \pm 2(2h/q)^{1/2} \tan^{-1}\{\exp[2(x - vt)/L]\}. \tag{A5}$$

References

Ali M K and Somorjai R L 1979 *J. Phys. A: Math. Gen.* **12** 2291
Batteh J H and Powell J D 1978 *J. Appl. Phys.* **49** 3933
Collins M A 1981 *Chem. Phys. Lett.* **77** 342
Collins M A and Rice S A 1982 *J. Chem. Phys.* **77** 2607
Earne Y Y and Weiner J H 1974 *J. Appl. Phys.* **45** 603
Fermi E, Pasta J and Ulam S 1965 *Collected Papers of Enrico Fermi* (Chicago: University of Chicago Press) paper 226, pp 978-88
Flytzanis N, Crowley S and Celli V 1977 *Phys. Rev. Lett.* **39** 891

Flytzanis N 1978 *Solitons and Condensed Matter Physics* ed A R Bishop and T Schneider (Berlin: Springer) p 166
Flytzanis N, Pnevmatikos St and Remoissenet M 1985 *J. Phys. C: Solid State Phys.* **18** 4603
—— 1987 *Physica* **26D** 311
Hardy J R and Karo A M 1978 *Lattice Dynamics* ed M Balkanski (Paris: Flammarion) p 163
Holian B L, Flaschka H and McLaughlin D W 1981 *Phys. Rev.* B **24** 2595
Ishimori Y 1982 *Prog. Theor. Phys.* **68** 402
Ishimori Y and Munakata T 1982 *J. Phys. Soc. Japan* **51** 3367
MacDonald R A and Tsai D H 1978 *Phys. Rep.* **46** 1
Mertens F G and Büttner H 1982 *J. Phys. A: Math. Gen.* **15** 1831
Mokross F and Büttner H 1983 *J. Phys. C: Solid State Phys.* **16** 4539
Peyrard M and Kruskal M D 1984 *Physica* **13D** 88
Peyrard M, Odiot S, Lavenir E and Schnur J M 1985 *J. Appl. Phys.* **57** 2626
Peyrard M, Pnevmatikos St and Flytzanis N 1986 *Physica* **19D** 268
Pnevmatikos St 1983 *C.R. Acad. Sci. Paris* II **296** 1031
—— 1985 *Singularities and Dynamical Systems* (*Math. Stud.* **103**) ed St Pnevmatikos (Amsterdam: North-Holland) p 397
Pnevmatikos St, Flytzanis N and Remoissenet M 1986 *Phys. Rev.* B **33** 2308
Powell J D and Batteh J H 1980 *J. Appl. Phys.* **51** 2050
Remoissenet M and Flytzanis N 1985 *J. Phys. C: Solid State Phys.* **18** 1573
Rolfe T J, Rice S A and Dancz J 1979 *J. Chem. Phys.* **70** 26
Rosenau P 1986 *Phys. Lett.* **118A** 222
Straub G K and Holian B L 1979 *Phys. Rev.* B **19** 4049
Tasi J 1980 *J. Appl. Phys.* **51** 5816
Toda M 1975 *Phys. Rep.* **18** 1
Tsai D H'and Trevino S F 1984 *J. Chem. Phys.* **81** 5636
Valkering T P and de Lange C 1980 *J. Phys. A: Math. Gen.* **13** 1607
Yoshida F and Sakuma T 1979 *Prog. Theor. Phys.* **61** 676
Zabusky N J 1973 *Comput. Phys. Commun.* **50** 1